A New Design of Optical Logic Gates with Transverse Electric and Magnetic

Lili Liu[1], Haiquan Sun[2*], Lishuang Hao[3], Cailiang Chen[4]
Xuanhua Vocational College of Science & Technology, Zhangjiakou Hebei, 075000, China[1, 3, 4]
Hebei University of Architecture, Zhangjiakou Hebei, 075000, China[2]

***Abstract*—This paper presents a new design of optical NOR and XNOR logic gates using a two-dimensional-hexagonal photonic crystal (2D-HPhC) that allows for both Transverse Electric (TE) and Transverse Magnetic (TM) polarization modes. The structure is very small in size and has a low delay time. The design includes three inputs (A, B, C) and one output (Q) waveguide, with the NOR gate having a delay period of 0.75 ps and the XNOR gate having a delay period of 0.9 ps. The contrast ratio between the input and output for both gates is 7-8 dB. The XNOR gate has an optimum transmission signal rate of T = 96%. The purpose of the structure is to use a reference input to create the fundamental logic gates NOR and XNOR by adjusting the signal phase angle.**

***Keywords*—Photonic crystal; hexagonal lattice; NOR; XNOR; transverse electric; transverse magnetic**

I. INTRODUCTION

Future electronic circuits will have speed constraints due to the growth of telecommunication systems to enhance the speed and bandwidth acceptable for data transfer (frequency). In optical networks and signal processing systems, high-frequency, all-optical logic gates are essential. All-optical logic switches and gates are among the basic components for designing future information processing systems and optical networks. Using optical networks, speed and capacity limits in communication networks are solved [1]. Optical crystals are considered a suitable structure in optically integrated circuits due to their compressibility. For the implementation of all-optical logic gates, several architectures have been suggested thus far. Logic gates through linear and nonlinear photonic crystals have gotten special attention in order to ease the integration of the suggested architectures [2]. A logic gate in a digital system executes a logical operation on one or more rationale inputs before producing a rationale yield. All digital circuits often employ Boolean logic, which is the foundation of this logic. Logic gates use binary logic, mostly made of transistors and diodes in electrical devices.

Photonic crystals are alternating structures on the nanoscale and affect the motion of photons due to changes in the refractive index of the components and the proportional wavelength. This is what semiconductor crystals do with electrons. Similar to how the Schrodinger equation involves electrical potential, the refractive index plays a part in the Helm-Holtz equation. The periodicity in the refractive index, more or less within the crystal, serves as the foundation for photonic crystals. The wavelength of the photons affects how they are emitted inside these structures. Modes are the light wavelengths that are permitted to move. A group of diffuse fashions forms the bandgap. Unauthorized bands of photonic crystals are called bandgaps. If we have materials of the dielectric material, which have a forbidden band for photons, at a certain frequency range no light can move inside the crystal structure of matter. The most important difference between photons and electrons is their velocity. Electrons belong to the group of fermions due to their incorrect spin, and the Pauli Exclusion Principle governs them. In contrast, photons have the correct spin and are considered bosons, so there is no limit to the number and energy of photons in the crystal. The effect of photons on each other is much less than the interaction of electrons, which reduces losses in dielectrics. Because the shrinkage of optical circuits faced problems such as energy loss, photonic crystals have been proposed to solve this problem. Defects in photon crystal structures can be created and based on the defects in the photon crystal lattice, these structures are divided into three categories: one-dimensional, two-dimensional, and three-dimensional [3].

Due to the use of photonic crystals to make all-optical logic gates and their use in all-optical systems, structures with low losses and high efficiency are required for all-optical logic gates. The proposed structure for all-optical logic gates based on photon crystals should have small dimensions (for integration), low losses, and a suitable distance between to be logic surfaces. In addition to the above, the working wavelengths of the proposed structure should be in telecommunication windows so that these logic gates can be used in filters, switches, sequential circuits, and all-optical composite circuits. Given the importance of processing speed, bandwidth, and dimensions in today's all-optical integrated circuits, it is necessary to provide a structure with such specifications. In this research, we will try to design and simulate a structure with the mentioned capabilities, and the proposed structure will be flexible and will change the type of logic gates with a small change in the arrangement of dielectrics. The initial structure proposed is the NOR logic gate, based on a photonic crystal, the subsequent gates being designed by trial and error and the experience of previous articles in the field.

Today, the demand for high bandwidth to reduce the speed limit of electronic devices is increasing rapidly. Optical signal processing requires complex logic gates. To build all-optical systems, it is necessary for all the components used to be able to work in the optical network. Gates are key components for building all-optical systems. In order to convert digital gates into all-light gates, changes in the original design are needed.

To design all-optical gates, it is necessary to apply an alternating layer of dielectrics, which modulates the signal to produce the desired results. Nonlinear effects can be achieved using various methods such as nonlinear ring mirrors, linear fiber, photon crystals, changing the refractive index of materials, filters, waveguides, or optical semiconductor amplifiers [4]. Optical elements that reduce the size of optical integrated circuits are good candidates for future optical networks and optical computations due to the transmitted wavelength. All-optical communication is one of the solutions to the problem of the speed and size of electronic circuits. Logic gates are one of the most important components in all-optical circuits. In recent years, researchers have developed all-optical logic gates for use in nonlinear effects in optical fibers, but one of the limitations has been a large size, low speed, and size of integrated circuits [5].

Many researchers have been interested in all-optical signal processing techniques recently, but all-optical devices must be fully utilized to use optical transmission capabilities. These devices include optical filters [6, 7], optical multiplexers [8, 9], optical analogue-to-digital converters [10, 11], optical switches [12], optical logic gates [13, 14], optical accelerometers [15], optical half-adders [16], and other similar optical devices. A device known as an "all-optical logic gate" produces logic outputs by performing logic operations on light with light. When one or more lights with light inputs are subjected to logic operations, the device is known as a logic gate. High-speed all-optical logic gates are necessary in the processing of signal as well as optical networks. The complication, speediness, reliability, steadfastness, and straightforwardness of integration of the numerous designs created hence distant to degree the execution of all-optical rationale gates shift. Rationale entryways based on through straight and nonlinear photon precious stones have gotten extraordinary consideration and have been significantly broadened to help in joining the recommended structures [17, 18]. All-optical rationale gates based on photon precious stones may be made, recreated, and fabricated utilizing nanocavity, nonlinear fabric characteristics, ring resonators, and the Mach Zehnder interferometer. On the premise of XOR, XNOR, NAND, and NOT rationale entryways, Nozhat et al. effectively outlined high-contrast nonlinear two-dimensional gem photonics in 2015. The tall differentiate proportion of around 20 dB between "1" and "0" [19] may be a recognizing quality of this rationale entryway in comparison to other rationale gates already formulated. A two-input, two-dimensional photon crystal-based NAND gate with a ring resonator was recommended by Siraj M. The proposition incorporates an add up to zone of 249.75µm2, and the delay time is, at best, 3.6 ps [16, 20]. Most newly suggested rationale entryway designs can as it were work within the TM or TE polarization modes. Both the delay time and the auxiliary estimate are significant.

Employing a hexagonal cross section in silicon photon gems on a cover and autonomous of polarization, a strategy for building all-optical rationale entryways is given in this inquire about. An assortment of entryways utilized in this way can join optical rationale gates through the obstructions wonders, utilizing direct blemishes and obstructions between light bars.

II. NUMERICAL METHODS

The finite difference time domain (FDTD) approach may demonstrate light diffusing in a photonic crystal. The center thought behind the limited contrast time space approach is to inexact spatial and worldly subsidiaries utilizing the limited contrast in Maxwell conditions. The microstructure under examination is split into a small number of constant lattice points in the FDTD technique, where the field values are computed. For the expression of spatial and temporal derivatives, magnetic and electric fields use backslash and anterior differences, respectively. For the electric and magnetic regions of Maxwell's Eq. (1) and (2), the derivatives listed below can be used in their place.

$$\frac{\partial E(r,t)}{\partial r_i} \to \frac{\Delta_i + \hat{E}}{\Delta r_i} = \frac{\hat{E}(r + q_i u_i, t) - \hat{E}(r,t)}{q_i} \tag{1}$$

$$\frac{\partial E(r,t)}{\partial t} \to \frac{\Delta_i + \hat{E}}{\Delta t} = \frac{\hat{E}(r,t+\delta t) - \hat{E}(r,t)}{\delta t} \tag{2}$$

$$\frac{\partial H(r,t)}{\partial r_i} \to \frac{\Delta_i - \hat{H}}{\Delta r_i} = \frac{\hat{H}(r,t) - \hat{E}(r - q_i u_i, t)}{q_i} \tag{3}$$

$$\frac{\partial H(r,t)}{\partial t} \to \frac{\Delta_i - \hat{H}}{\Delta t} = \frac{\hat{H}(r,t) - \hat{H}(r,t-\delta t)}{\delta t} \tag{4}$$

In these equations, qi denote distance among the grid's lattice points and ui the unit vectors that constitute the computational grid, are used to measure the geometric space. Reclaimed by fields:

$$\hat{E} = q_i E \to and \to \hat{H} = q_i H \tag{5}$$

The x and z axes of the FDTD simulator's coordinate system are specified to lie in $\Gamma - M$ and $\Gamma - k$ planes, correspondingly. The direction of y is vertical/perpendicular to crystal's surface for fitting the hexagonal configurations' geometry. The rectangular coordinate is regarded for the lattice coordination where the distance of lattice is considered $qx = \sqrt{3}.qz$. The FDTD software accordingly ensures stability.

$$\delta t = 0.99\sqrt{\frac{3}{7}}\left(\frac{q_x}{c}\right) \tag{6}$$

Where qx denotes the x-directional lattice distance, the relationship between the spatial grid and worldly steps is illustrated by the statement mentioned above, which states that for a more precise spatial lattice, numerous more worldly steps are vital. The output contrast ratio is yet another factor of significance in the development of logic gates [21]. The ratio of the control for "1" rationale to the control for "0" rationale from the condition is utilized to compute the differentiate proportion for both TE and TM polarizations.

$$\text{ContrasrRatio(CR)} = 10 \log (P_1/P_0)(\text{dB}) \tag{7}$$

Where P0 stands for the control of the consistent "0," whereas P1 speaks to the coherent control of "1." In this work, we decide the differentiate proportion for this rationale gate at 1.550 µm wavelength.

III. PHOTONIC BAND STRUCTURE

The behavior of light as it passes through a periodic structure, which generates a number of potential barriers and wells for photons, is referred to as the photonic band structure. Similar to the energy bands for electrons in a solid, the structure produces photonic bands and energy gaps known as photonic band gaps. In order to ascertain the band structure and operating wavelength of photonic structures, it is essential to comprehend the microstructure of photonic bandgap graphs. The band structure of the in-demand unit cell depends on the microstructure of the photonic bandgap graph. In order to create photonic crystals with distinctive optical characteristics, the photonic band structure and the microstructure of photonic bandgap graphs are crucial.

Here, the microstructure of the photonic bandgap graph has been selected to begin with some time recently continuing to the specifics of the plan and displaying. Getting the recurrence crevice is one of the key thoughts within the microstructure of vitality groups. The working wavelength is the wavelength that can be exchanged from the source to the yield without being scattered, losing vitality, or entering the structure. According to Blah's theory, this requires knowledge of the microstructure's unit cell. The hexagonal photonic crystal's unit cell is seen in Fig. 1.

In arrange to decide the in-demand unit cell's band structure, we must to begin with decide the structure's unit cell. The bandgap structure is seen in Fig. 2. The recommended microstructure within the wavelength run of λ = 1.4874μm ~ 1.621μm as appeared, and encompasses a full photonic bandgap within the normalized recurrence run of a λ = 0.3516 ~ 0.3832.

Remember that the structure has a complete bandgap since the specified gates are polarization-independent. The bandgaps for the TM and TE modes cross across, as seen in the above picture.

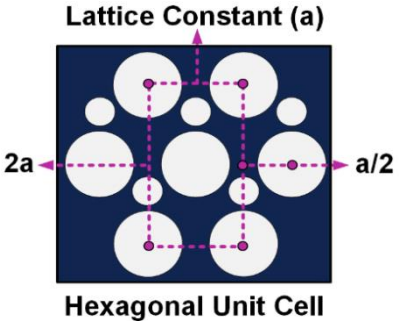

Fig. 1. The hexagonal cell of the planned rationale entryways.

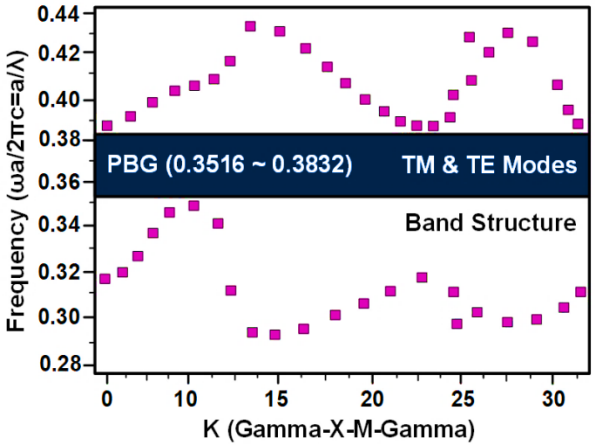

Fig. 2. Photonic band structure.

IV. OPTICAL LOGIC GATE

In expansion to the two essential inputs, another input is included within the plan of rationale entryways to alter the application and increment the applications, such as NOR and XNOR. This extra input permits fluffy control of the optical signals. So, when there are three input waveguides and one yield waveguide, the suggested structure is as takes after. (Fig. 3) The performance of the constructive and destructive interference in the controller waveguide results in the logic gates. On the SOI substrate, the recommended plan comprises of an $X \times Z$ hexagonal cross section with a number of 17×15 gaps separated into two bunches. The sweep was selected to produce two diverse photonic bandgaps. The two air holes have a radius of $r_b = 0.36a$ for the larger air hole and $r_s = 0.16a$ for the smaller air hole, where (a) is the cross-section steady, which is equivalent to a=550 nm. The greater air holes are completely in the middle of the smaller ones. The two-dimensional photonic crystal's holes are partially removed to produce the waveguides. Using the effective refractive index approach, two-dimensional analysis is carried out since three-dimensional computations take more time and memory.

$n(TM) = 2.150$ and $n(TE) = 2.890$ and, respectively are determined as the successful chunk refractive records for the TE and TM modes at the wavelengths=1.550μm. The suggested design has been determined to be capable of acting as all-optical logic gates after the microstructure has been tuned for both polarization modes at wavelength.

The suggested structure has four waveguides that serve as input and output ports for designing and simulating all-optical rationale gates with three inputs. The two major input ports are the Q output and a C reference or Controller input. Depending on the staging point, the port's reference signal or control indicator generates a stage contrast between the input indicators, coming about in either helpful or dangerous obstructions between the input indicators. Since the symmetry of the reflect picture around the waveguides, most light is caught in this construction's waveguide locale. Also, the input and yield waveguide borders are changed by the incorporation of more discuss gaps with lower radii. An enormous discuss gap and two littler discuss gaps maximize the optical control transmission. This method has impressive focal points for optical control transmission to the yield and avoiding optical control misfortune within the structure. Within the following step of the plan, four waveguides with a gap within the center are proposed. Again, this gap is tuned for both TM and TE modes with a polarization-dependent central gap sweep of 0.23. When combined with the reference flag, both input signals provide the highest possible value for TM and TE polarizations, making this sweep ideal for the input flag. The most effective regulation happens once one of the two input signals is propagated on two input waveguides at once, leading to light-generating impedances at the junction of four waveguides when all of the signals are onstage. Since dangerous impedances happens when the signals are out of stage, the portrayed strategy may be utilized to execute the NOR and XNOR optical rationale gates. Less control will be shown within the yield waveguide as a result.

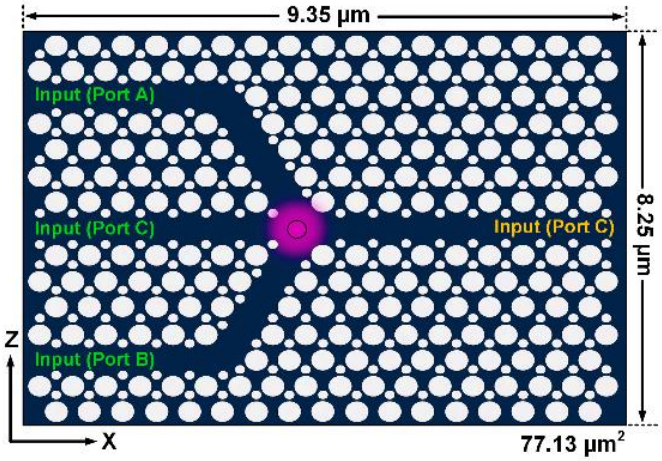

Fig. 3. The proposed of 2D-HPhC structure.

V. Result and Discussion

There are three different kinds of general logic operations that will be executed in this suggested architecture. If a light signal with φ = 0° is applied to either the A or B input port and a control signal with φ = 0° is applied to the reference port, then a logical "1" is produced. When a light signal with a φ = 0° is excited at either the A or B input port and the reference port is stimulated with a control signal with a φ = π°, a logical "0" is produced. And, the highest output power is achieved when the reference port is activated only by the controller signal at either φ = 0° or φ = π° out of phase.

A. NOR Optical Logic Gate

The NOR logic gate, primarily employed in most digital devices' design, follows the reverse OR gate. Four separate states are used to characterize the NOR logic gate's operation [19, 21]. Table I displays this logic gate's potential states and the transmission rate.

Within the 'to begin with' situation, no flag is connected to any of the input ports, and the control flag is connected to the reference harbour with a stage point of $\varphi = \pi°$. When utilizing TE or TM polarization, the yield harbour, in this occasion, gets "1" rationale at a transmission rate of 67% or 58%, separately. The reference harbour is concurrently energized with the light flag with a stage point of φ = π° and the control flag by a stage point of 180 degrees ($\varphi = \pi°$) within the moment and third occurrences, separately, and *A* and *B* input ports are energized concurrently by the light flag within the moment and third cases. Fig. 4 portrays the introductory state. As watched, the TE-polarization mode has the most reduced delay time or the fastest working speed with a NOR Entryway within the moment state, 0.75ps.

Segments (a) and (b) of Fig. 5 show the field conveyance designs for the TE and TM polarization modes, individually. The consequences illustrate that the planned strategy capacities as a NOR optical rationale gate.

This gate has a signal in each of its reference ports at an angle of 180 degrees (φ=π°), as observed. Also, 7dB is used for the contrast parameter.

B. Optical Logic Gate of XNOR

Within the 'to begin with' state, no flag is connected to any input ports, whereas the control flag is connected to the reference harbour with a stage point of $\varphi = 0°$ [18]. Within the moment and third stages, a light flag with a stage point of $\varphi = 0$ is used to individually excite the A as the input port and, subsequently, the second input port B. In contrast, a control signal by a phase angle of $\varphi = \pi°$ is utilized to exclusively energize the primary input harbour A and, hence, the moment input harbour B. In differentiate, a control flag with a stage point of $\varphi = 0°$ fortifies A and B i.e., input ports and reference harbour C within the fourth state. In this occurrence, constructor obstructions is fulfilled since all three light signals are at co-phase in yield harbour 1. Table II lists the findings for every possible combination of TM and TE polarizations. At 1550 nm wavelengths, the difference percentage for this reasonable entrance is 8dB.

The three fundamental states within the TE and TM polarization modes are appeared within the field dissemination in Fig. 6(a) a persistent Gauss a wavelength of 1550 nm. Section (a), which can be seen in the image, simulates the three principal states while applying an optical signal source in TE mode to the microstructure. The inputs in the section receive an optical signal source operating in TM mode (b).

The reenactment discoveries appear that the stage alter point of the reference harbour C is utilized to construct all of the elemental optical rationale entryways utilized in optical coordinates circuits. Another significant benefit of the suggested microstructure is its ability to receive polarization and supply the correct output. The TE-polarization modes and the TM-polarization mode's respective minimum delay times are one period (ps) and nine periods (ps), respectively.

TABLE I. THE PRECISION RESULTS OF THE NOR LOGIC GATE

(Q)	0	1	0	0
T (TE Mode)	5 %	65 %	11 %	5 %
T (TM Mode)	5 %	58 %	6 %	5 %
Input (A)	0i(φ=0°)	0i (φ=0°)	1i (φ=0°)	1i (φ=0°)
Input (B)	1i (φ=0°)	0i (φ=0°)	1i (φ=0°)	0i (φ=0°)
Input (C)	1i (φ= π°)	1i (φ= π°)	1i (φ= π°)	1i (φ= π°)

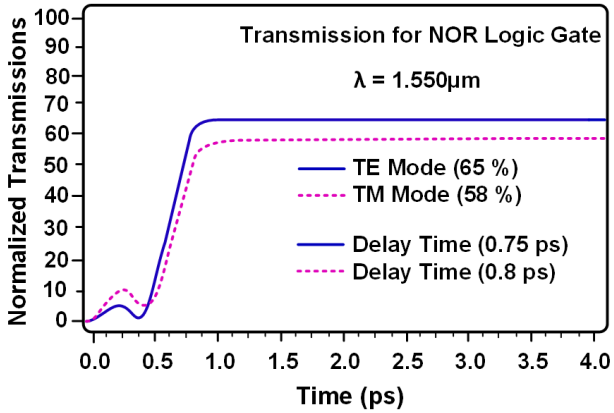

Fig. 4. The time of delay for second state of NOR logic gate.

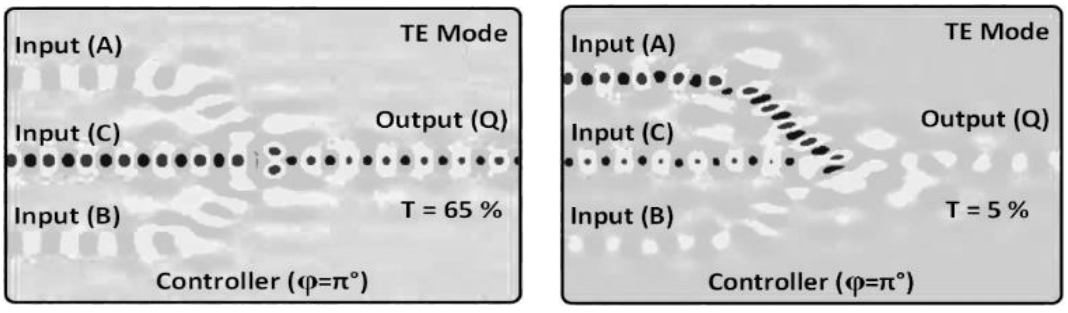

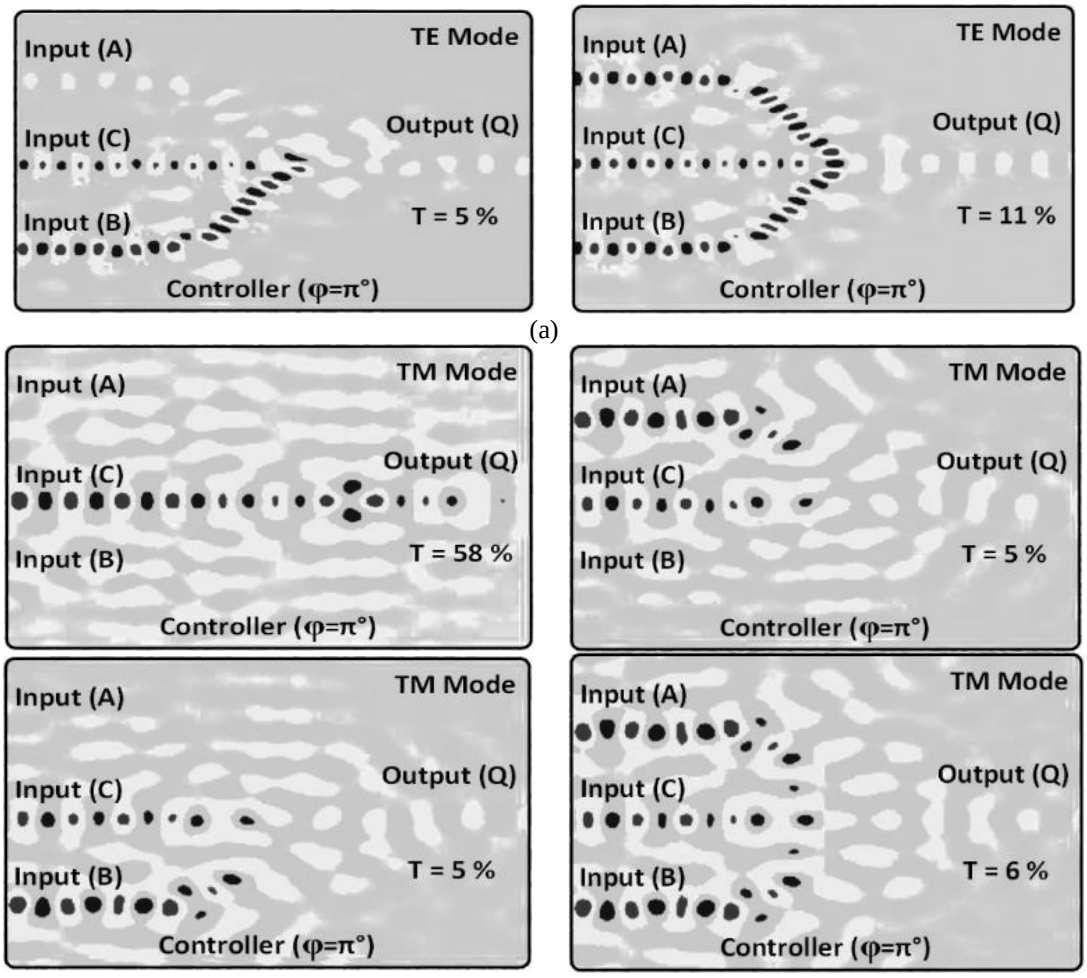

Fig. 5. Field dissemination at NOR rationale entryway, (a) TE mode, (b) TM mode.

TABLE II. THE EXACT NECESSITY OF THE NOR RATIONALE GATE WITH FOUR INPUTS.

(Q)	**0**	**1**	**1**	**0**
T (TE Mode)	5 %	64 %	96%	5%
T (TM Mode)	5 %	58 %	90 %	5%
Input (A)	0i (φ=0°)	0i (φ=0°)	1i (φ=0°)	1i (φ= 0°)
Input (B)	1i (φ=0°)	0i (φ=0°)	1i (φ=0°)	0i (φ=0°)
Input (C)	1i (φ= π°)	1i (φ= π°)	1i (φ=0°)	1i (φ= π°)

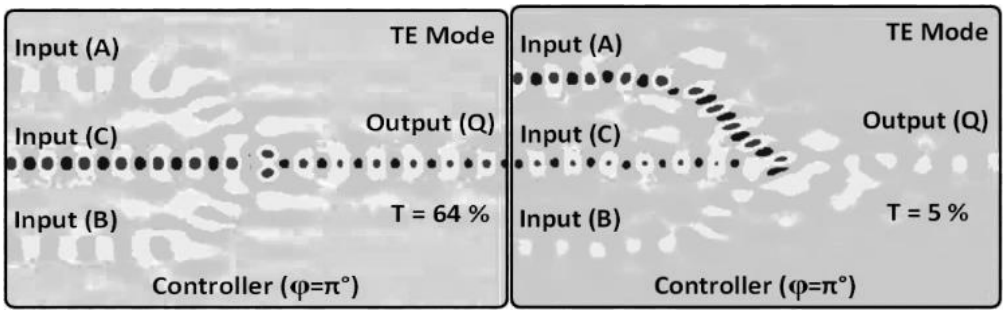

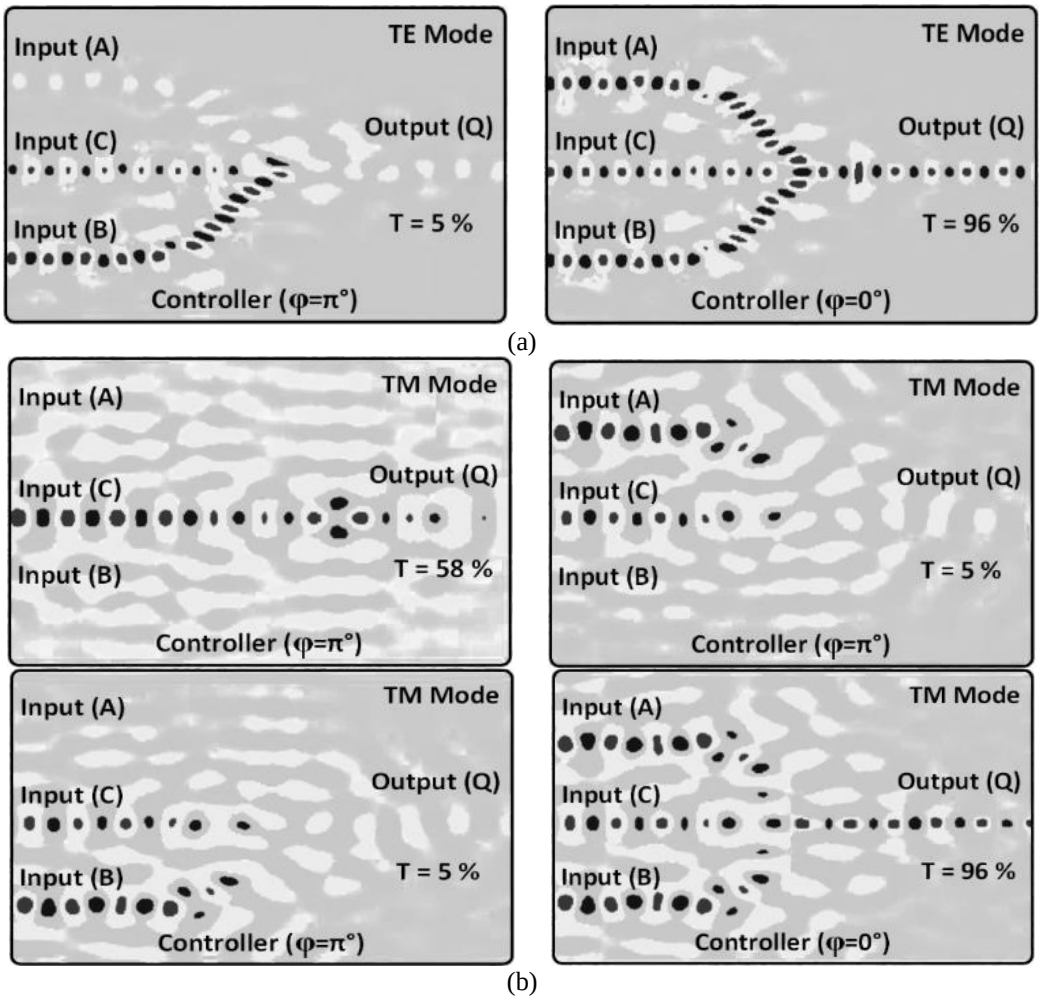

Fig. 6. Field dispersion at XNOR rationale gate, (a) TE mode, (b) TM mode.

VI. CONCLUSION

This paper plans and mimics all base rationale gates (TE/TM) free of polarization modes utilizing a hexagonal photonic gem with silicon dielectric on a separator. Embracing the recommended microstructure will empower the headway of all prior thinks about to a brand-new era of polarization-independent gates. In this paper, a novel optical NOR and XNOR logic gate design is introduced utilizing a two-dimensional-hexagonal photonic crystal (2D-HPhC) that facilitates Transverse Electric (TE) and Transverse Magnetic (TM) polarization modes. The size of the structure is relatively small, and it possesses a low delay time. The design incorporates a waveguide with three inputs (A, B, C) and one output (Q). The NOR gate demonstrates a delay period of 0.75 ps, while the XNOR gate showcases a delay period of 0.9 ps. The contrast ratio between input and output for both gates is 7-8 dB. Furthermore, the XNOR gate displays an optimal transmission signal rate of T = 96%. The work of hexagonal photonic gems, silicon dielectric fabric on cover with a satisfactory thickness, and the span of the gaps within the structure causes the mutual bandgap in equally TM and TE polarization types. The current study is only considered the specific design and parameters of the gates and does not explore other possible configurations or applications of the 2D-HPhC. Future study could explore the potential of integrating the 2D-HPhC design with other technologies for advanced functionality and performance.

REFERENCES

[1] Q Gong, X Hu, editors, "Photonic crystals," principles and applications. CRC Press. 6, (2014).

[2] K Arunachalam, SC Xavier. Optical logic devices based on the photonic crystals," Photonic crystals introduction, applications and theory. 30, pp.63-80, (2012).

[3] S. Noda, K. Tomoda, N. Yamamoto, and A. Chutinan, "Full Three-Dimensional Photonic Bandgap Crystals at Near-Infrared Wavelengths," Science, 289, pp. 604-606, (2000).

[4] A. P. Kabilan, X. S. Christina and P. E. Caroline, "Photonic Crystal Based All-Optical or and Xo Logic Gates," in 2010 Second International Conference on Computing, Communication, and Networking Technologies, pp. 1-4. (2010).

[5] S. Swarnakar, S. Kumar, S. Sharma, and L. Singh, "Design of XOR/and Gate Using 2D Photonic Crystal Principle," in SPIE OPTO, Vol. 10130, pp. 162-172, pp. 11. (2017).

[6] M. Hosseinzadeh Sani, A Ghanbari, and H Saghaei. "An ultra-narrowband all-optical filter based on the resonant cavities in rod-based photonic crystal microstructure," Optical and Quantum Electronics 52, pp.1-15. (2020).

[7] M. Youcef Mahmoud, G. Basso, A. Taalbi and Z. M. Chekroun, "Optical Channel Drop Filters Based on Photonic Crystal Ring Resonators", Optics Communications, 285, pp.368-372, (2012).

[8] H. Alipour-Banaei, F. Mehdizadeh and S. Serajmohammadi, "A Novel 4-Channel Demultiplexer Based on Photonic Crystal Ring Resonators", Optik - International Journal for Light and Electron Optics, 124, pp. 5964-5967, (2013).

[9] M. Reza Rakhshani and M. Ali Mansouri-Birjandi, "Design and Simulation of Wavelength Demultiplexer Based on Heterostructure Photonic Crystals Ring Resonators", Physica E: Low-dimensional Systems and Nanostructures, 50, pp. 97-101, (2013).

[10] M H Sani, S Khosroabadi., & A Shokouhmand,A novel design for 2-bit optical analog to digital (A/D) converter based on nonlinear ring resonators in the photonic crystal structure. Optics Communications, 458, 124760. (2020).

[11] M H Sani, M Hosseinzadeh, S Khosroabadi, and M Nasserian. "High performance of an all-optical two-bit analog-to-digital converter based on Kerr effect nonlinear nanocavities." Applied optics 59. 4. (2020). pp.1049-1057.

[12] T. Ahmadi Tameh, B. M. Isfahani, N. Granpayeh, and A. M. Javan, "Improving the Performance of All-Optical Switching Based on Nonlinear Photonic Crystal Microring Resonators", AEU - International Journal of Electronics and Communications (2011)., 65, pp. 281-287.

[13] P. Andalib and N. Granpayeh, "All-Optical Ultracompact Photonic Crystal and Gate Based on Nonlinear Ring Resonators", Journal of the Optical Society of America B, (2009).26, pp.10-16.

[14] P Sami, Ch Shen, and M Hosseinzadeh Sani. "Ultra-fast all-optical half-adder realized by combining AND/XOR logical gates using a nonlinear nanoring resonator." Applied Optics. (2020).59.22. pp.6459-6465.

[15] M Hosseinzadeh Sani, et al. "A novel all-optical sensor design based on a tunable resonant nanocavity in photonic crystal microstructure applicable in MEMS accelerometers." Photonic Sensors (2021).11.4. pp.457-471.

[16] M. H Sani., A. A Tabrizi, H Saghaei & R Karimzadeh,. An ultrafast all-optical half adder using nonlinear ring resonators in photonic crystal microstructure. Optical and Quantum Electronics, (2020) 52(2), pp.1-10.

[17] Z.-H. Zhu, W.-M. Ye, J.-R. Ji, X.-D. Yuan and C. Zen, "High-Contrast Light-by-Light Switching and Gate Based on Nonlinear Photonic Crystals", Optics Express, (2006)14, pp. 1783-1788.

[18] Y. J. Jung, S. Yu, S. Koo, H. Yu, S. Han, N. Park, "Reconfigurable All-Optical Logic and, Nand, or, nor, Xor and XNOR Gates Implemented by Photonic Crystal Nonlinear Cavities," in Conference on Lasers and Electro-Optics/Pacific Rim, Shanghai, p. TuB. (2009), pp.4_3.

[19] Z. Mohebbi, N. Nozhat and F. Emami, "High Contrast All-Optical Logic Gates Based on 2d Nonlinear Photonic Crystal", Optics Communications, (2015) 355, pp. 130-136.

[20] S Serajmohammadi,. and H. Absalan, all-optical NAND gate based on nonlinear photonic crystal ring resonator, Information processing in Agriculture, (2016). 3(2), pp. 119-123.

[21] A Mohebzadeh-Bahabady, and S. Olyaee, All-optical NOT and XOR logic gates using photonic crystal nano-resonator and based on an interference effect, IET Optoelectronics, (2018). 12(4), pp. 191-195.